
Since January 2020 Elsevier has created a COVID-19 resource centre with free information in English and Mandarin on the novel coronavirus COVID-19. The COVID-19 resource centre is hosted on Elsevier Connect, the company's public news and information website.

Elsevier hereby grants permission to make all its COVID-19-related research that is available on the COVID-19 resource centre - including this research content - immediately available in PubMed Central and other publicly funded repositories, such as the WHO COVID database with rights for unrestricted research re-use and analyses in any form or by any means with acknowledgement of the original source. These permissions are granted for free by Elsevier for as long as the COVID-19 resource centre remains active.

International Immunopharmacology 93 (2021) 107317

Contents lists available at ScienceDirect

International Immunopharmacology

journal homepage: www.elsevier.com/locate/intimp

# Ergosterol peroxide exhibits antiviral and immunomodulatory abilities against porcine deltacoronavirus (PDCoV) *via* suppression of NF-κB and p38/MAPK signaling pathways *in vitro*

Cong Duan [a], Xinna Ge [a], Junchi Wang [b], Zhanyong Wei [c], Wen-hai Feng [d,*], Jiufeng Wang [a,*]

[a] College of Veterinary Medicine, China Agricultural University, Beijing 100193, China
[b] Institute of Medicinal Plant Development, Chinese Academy of Medical Sciences and Peking Union Medical College, Beijing 100193, China
[c] College of Animal Science and Veterinary Medicine, Henan Agricultural University, Zhengzhou 450002, Henan, China
[d] State Key Laboratory for Agrobiotechnology, College of Biological Science, China Agricultural University, Beijing 100193, China

ARTICLE INFO

*Keywords:*
Porcine deltacoronavirus
Ergosterol peroxide
Antiviral agents
NF-κB signaling pathway
p38/MAPK signaling pathway

ABSTRACT

Porcine deltacoronavirus (PDCoV) is an emerging swine enteropathogenic coronavirus (CoV) that poses economic and public health burdens. Currently, there are no effective antiviral agents against PDCoV. *Cryptoporus volvatus* often serves as an antimicrobial agent in Traditional Chinese Medicines. This study aimed to evaluate the antiviral activities of ergosterol peroxide (EP) from *C. volvatus* against PDCoV infection. The inhibitory activity of EP against PDCoV was assessed by using virus titration and performing Quantitative Reverse transcription PCR (RT-qPCR), Western blotting and immunofluorescence assays in LLC-PK1 cells. The mechanism of EP against PDCoV was analyzed by flow cytometry, RT-qPCR and Western blotting. We found that EP treatment inhibited PDCoV infection in LLC-PK1 cells in a dose-dependent manner. Subsequently, we demonstrated that EP blocked virus attachment and entry using RT-qPCR. Time-of-addition assays indicated that EP mainly exerted its inhibitory effect at the early and middle stages in the PDCoV replication cycle. EP also inactivated PDCoV infectivity directly as well as suppressed PDCoV-induced apoptosis. Furthermore, EP treatment decreased the phosphorylation of IκBα and p38 MAPK induced by PDCoV infection as well as the mRNA levels of cytokines (IL-1β, IL-6, IL-12, TNF-α, IFN-α, IFN-β, Mx1 and PKR). These results imply that EP can inhibit PDCoV infection and regulate host immune responses by downregulating the activation of the NF-κB and p38/MAPK signaling pathways *in vitro*. EP can be used as a potential candidate for the development of a new anti-PDCoV therapy.

## 1. Introduction

Porcine deltacoronavirus (PDCoV), belonging to the genus *Deltacoronavirus* of the family *Coronaviridae*, is a widespread swine enteropathogenic coronavirus (CoV), which can cause severe dehydration, vomiting and watery diarrhea in piglets [1]. Since its first detection in 2012 in pig feces [2], PDCoV has subsequently been found in a number of countries, including the USA, South Korea, Japan, Canada and China [1,3–6]. In addition, PDCoV can infect a variety of animals, exhibiting a wide range of tissue tropisms. Studies have found that PDCoV can also infect calves, chickens and turkeys [7–9], highlighting its ability to cross interspecies barriers. The global distribution of PDCoV in pigs and its potential for transmission to various hosts are alarming. Pigs are intermediate hosts for several pathogens that can be transmitted zoonotically, which underscores the need for studying the zoonotic potential of PDCoV and the development of antiviral drugs against it [10].

Until now, there have been no effective therapeutics or vaccines to control PDCoV infections. The currently used antiviral agents have significant side effects and lead to the development of drug resistance in virus population because the virus is evolving under selective pressures [11]. Due to the lack of specific antiviral therapies to control PDCoV infections, it is important to find effective small-molecule inhibitors that are active against PDCoV. Natural products, which have intrinsic antiviral activities, are candidates to be developed as new generations of antivirals administrated either alone or in combination with current modalities [12].

In Asian countries, the medical use of mushrooms has a long

* Corresponding authors at: College of Biological Science, China Agricultural University, Beijing 100193, China (W.-H. Feng). College of Veterinary Medicine, China Agricultural University, Beijing 100193, China (J. Wang).
*E-mail addresses:* whfeng@cau.edu.cn (W.-h. Feng), jiufeng_wang@hotmail.com (J. Wang).

https://doi.org/10.1016/j.intimp.2020.107317
Received 17 September 2020; Received in revised form 10 December 2020; Accepted 15 December 2020
Available online 22 January 2021
1567-5769/© 2020 Elsevier B.V. All rights reserved.

tradition and this trend has become increasingly popular in the Western Hemisphere [13]. Our previous studies have shown that the extract of the mushroom *Cryptoporus volvatus* has anti-porcine reproductive and respiratory syndrome virus (PRRSV) and anti-influenza virus activities *in vivo* and *in vitro* [14,15]. Furthermore, ergosterol peroxide (EP) is abundant in *C. volvatus* and previous studies have shown that EP exhibits multiple biological properties, including antimicrobial, antitumorigenic and immunomodulatory activities [16,17]. However, whether EP has anti-PDCoV properties has yet to be determined.

The innate immune system is an evolutionarily conserved system of host defense against microbial infections. Cytokines are parts of the necessary initial immune response to pathogens. The activation of NF-κB is one of the hallmarks of a cell's response to invasion by different pathogens, which can be involved in the expression of cytokines [18]. The mitogen-activated protein kinase (MAPK) signaling pathway is another important signaling pathway related to viral infections [19]. The MAPK signaling pathway may regulate viral infections via single or multiple steps in the infection cycle. For example, ERK-2 regulates human immunodeficiency virus type 1 (HIV-1) assembly and release by phosphorylating the $p6^{gag}$ protein of HIV-1 [20] Inhibition of p38 or JNK1/2 results in a significant reduction of porcine epidemic diarrhea virus (PEDV) RNA synthesis, protein expression and progeny release [21]. Currently, numerous drugs have antiviral and anti-inflammatory activities mediated by regulating the activities of the NF-κB and MAPK signaling pathways, such as the anti-severe acute respiratory syndrome coronavirus 2 (SARS-CoV-2) effect of Liu Shen capsules [22].

In the present study, we investigated whether EP from the fruiting body of *C. volvatus* could inhibit PDCoV infection and elucidated the possible antiviral mechanism of EP *in vitro*.

## 2. Materials and methods

### 2.1. Preparation of ergosterol peroxide

*C. volvatus* was purchased from a market in Yunnan Province, China. The mushroom was authenticated, and a voucher specimen was deposited in our laboratory. Extraction and purity determination of EP were done as previously described [23]. Air-dried fruiting bodies of *C. volvatus* (1,200 g) were smashed and extracted with 90% ethanol 3 times under reflux for 1 h. The solvent was removed under reduced pressure to yield approximately 310 g of the ethanol extract, which was then suspended in water and partitioned with petroleum ether, dichloromethane, ethyl acetate and n-butanol. The dichloromethane fraction (250 g) was separated into eleven fractions (I-XI) by silica gel chromatography and eluted using dichloromethane-methanol (1:0–0:1, v/v). Fraction I (2.2 g) was then subjected to silica gel chromatography and eluted with petroleum ether-ethyl acetate (1:0–0:1, v/v) to obtain about 30 mg ergosterol peroxide with a purity of over 97%.

### 2.2. Virus propagation in LLC-PK1 cells

LLC-PK1 cells (ATCC CL-101) and ST cells (ATCC CRL-1746) were obtained from the American Type Culture Collection (ATCC) and cultured in MEM (Gibco, USA) supplemented with 1% antibiotic-antimycotic (Gibco, USA), 1% HEPES (Gibco, USA), 1% MEM non-essential amino acids solution (NEAA) (Gibco, USA) and 10% heat-inactivated fetal bovine serum (FBS) (Gibco, Australia). The maintenance medium for PDCoV propagation was MEM supplemented with 10 μg/mL trypsin (Gibco, USA) and cells were grown in a 5% $CO_2$ incubator. The PDCoV CHN-HN-1601 strain (GenBank accession no: MG832584) was provided by Professor Hanchun Yang, China Agricultural University, Beijing, China.

Virus propagation was performed as previously described [24]. Briefly, the cells were cultured in T75 flasks and washed twice with the maintenance medium at 80% confluency. The PDCoV CHN-HN-1601 strain in the maintenance medium was added to the flask. The cells were cultured continuously at 37 ℃ in 5% $CO_2$, and cytopathic effects (CPE) were monitored. When CPE was evident, the plates were frozen at −80 ℃ and thawed twice. The cells and supernatants were harvested together to determine viral titers. Viral titers were calculated using the Reed-Muench method [25] and expressed as $TCID_{50}$/mL.

### 2.3. Virus titration

LLC-PK1 cells were seeded into 96-cell plates and grown to 100% confluence for 24 h. Then, viral samples were serially diluted (10-fold) in MEM with 10 μg/mL trypsin and added to the LLC-PK1 cells in eight replicates per dilution. The cells were cultured continuously at 37 ℃ in 5% $CO_2$, and viral CPE was observed for 96 h. The viral titers are reported as $TCID_{50}$ calculated using the method of Reed and Muench.

### 2.4. Cytotoxicity assay

The cytotoxicity of EP was assessed *in vitro* using the Cell Counting Kit-8 (CCK8, DOJINDO, Japan) according to the manufacturer's instructions. LLC-PK1 cells were seeded into 96-cell plates and grown to 100% confluence for 24 h. After washing 3 times with phosphate-buffered saline (PBS), the cells were treated with increasing EP concentrations ranging from 3.9 to 248 μM. Mock-treated cells were used as control. After 36 h, the cells were washed with PBS and incubated with 100 μL MEM and 10 μL CCK8 solution at 37 ℃ for 2 h. Absorbance was measured with a microplate reader (Model 680 Microplate Reader, BIO-RAD, USA) at 450 nm. Cytotoxicity was analyzed according to the following formula:

$$\text{Cytotoxicity (\%)} = [(\text{Abs sample}) - (\text{Abs blank})]/[(\text{Abs negative control}) - (\text{Abs blank})] \times 100$$

### 2.5. Indirect immunofluorescence assay (IFA)

The cells were fixed with cold methanol-acetone (1:1, v/v) for 30 min at 4 ℃ and then permeabilized with 0.2% Triton X-100 in PBS for 10 min. After washing with PBS, the cells were blocked with 1% bovine serum albumin (BSA) for 45 min at 37 ℃. Subsequently, the cells were stained with anti-PDCoV monoclonal antibody (1:1000, provided by Professor Pinghuang Liu, China Agricultural University, Beijing, China) at 4 ℃ for 12 h. The cells were then washed and incubated with FITC-conjugated goat anti-pig IgG (1:200, Solarbio, China) for 45 min at 37 ℃. After 3washes with PBS, the cells were incubated with DAPI (1:1000, diluted in PBS) at room temperature for 5 min and examined by fluorescence microscopy (Olympus IX71, Tokyo, Japan).

### 2.6. Antiviral assay

To assess the antiviral efficacy of EP on PDCoV replication, confluent cells were inoculated with PDCoV (MOI = 0.5) in the presence of nontoxic concentrations of EP at 37 ℃ for 24 h. Ribavirin, a broad-spectrum antiviral drug, has previously been reported to inhibit Middle East respiratory syndrome coronavirus (MERS-CoV) replication (belonging to the same family as a novel CoV) [26], was used as a positive control. As a negative control, another set of cells was infected with the same amount of PDCoV without any drug treatment. After 24 h, the supernatants were collected for virus titration. In addition, the cells were fixed for IFA and the cell lysates were harvested for Quantitative Reverse transcription PCR (RT-qPCR) and Western blotting analysis.

### 2.7. Analysis of the effect of ergosterol peroxide on viral attachment

LLC-PK1 cells were seeded into 12-well plates and grown to 90% confluence for 24 h. EP at concentrations of 248 μM and 124 μM was mixed with the virus (MOI = 0.5), and the mixture was then added to the cells, followed by incubation for 1 h at 4 ℃. As a control, the cells were

infected with the same amount of PDCoV without any drug treatment. After washing with cold PBS, cell lysates were harvested for RT-qPCR analysis.

### 2.8. Analysis of the effect of ergosterol peroxide on viral entry

LLC-PK1 cells were infected with PDCoV (MOI = 0.5) at 4 ℃ for 1 h. Unbound viruses were removed by washing with cold PBS. The cells were then incubated with nontoxic EP (248 or 124 μM) at 37 ℃ for 1 h. As a control, another set of cells was infected with the same amount of PDCoV without any drug treatment. After removing the uninternalized viral particles on the cell surface by washing with acidic PBS-HCl (pH 3.0), cell lysates were harvested for RT-qPCR analysis.

### 2.9. Analysis of the effect of ergosterol peroxide on the post-entry stage of PDCoV life cycle

LLC-PK1 cells were infected with PDCoV (MOI = 0.5) at 4 ℃ for 1 h. Unbound viruses were removed by washing with cold PBS. After incubating at 37 ℃ for 1 h, the cells were then incubated with different concentrations of EP at 37 ℃ for 6 h. The supernatants were collected for virus titration, the cells were fixed for IFA and the cell lysates were harvested for RT-qPCR analysis.

### 2.10. Time-of-addition assay

Confluent LLC-PK1 cells were inoculated with PDCoV (MOI = 0.5) at 4 ℃ for 1 h, washed with cold PBS and then shifted to 37 ℃ (this time point was set up as 0 h). Different concentrations of EP (248 or 124 μM) were added at the time intervals of 1–3, 3–5 and 5–7 h post infection (hpi). The cells were fixed for IFA, and the cell lysates were harvested for RT-qPCR analysis.

### 2.11. Analysis of the viricidal effect

PDCoV (MOI = 0.5) was incubated with different concentrations of EP for 2 h at 37 ℃. The samples were then washed with 1 mL PBS, and re-purification was done using ultracentrifugation through a 20% (w/w) sucrose cushion at 90,000 g for 1.5 h at 4 ℃. The pelleted virions were re-suspended in PBS. Then, viral infectivity was determined by RT-qPCR, $TCID_{50}$ and IFA in LLC-PK1 cells.

### 2.12. Analysis of apoptosis

Apoptosis was analyzed using the Dead Cell Apoptosis Kit with Annexin V Alexa Fluor™ 488 & Propidium Iodide (PI) (Invitrogen, USA) by flow cytometry. Annexin V has a high affinity for the membrane phosphatidylserine, which is translocated from the inner face of the plasma membrane to the cell surface at the early stage of apoptosis. Therefore, FITC-labeled Annexin V can be used as a fluorescent probe to detect early cell apoptosis. Propidium iodide (PI) can pass through the membrane of apoptotic and necrotic cells and can be used to detect late apoptosis. Thus, a combination of Annexin V and PI can be used to distinguish early and late cell apoptosis.

In brief, LLC-PK1 cells were detached using trypsin (without EDTA) for 2 min and then centrifuged (1,000 × g, 5 min). The cells were washed twice with PBS and re-suspended with 100 μL of binding buffer. Then, 5 μL of Alexa Fluor 488 Annexin V and 1 μL of 100 μg/mL PI were added to the cells, followed by incubation at room temperature for 15 min in the dark and examination by a flow cytometer (BD FACSCalibur Flow Cytometer, BD Biosciences, CA, USA).

### 2.13. RNA extraction and RT-qPCR

Total RNAs from LLC-PK1 cells were extracted using TRIzol reagent (Invitrogen, USA). The RNAs were converted to cDNA using the HiFiScript cDNA Synthesis Kit (CoWin Biosciences, China). Viral RNA was analyzed using absolute quantitative RT-PCR with primers designed according to the PDCoV Spike (S) gene (Forward: CGTTAACCTCTTCTCACCACTT, Reverse: GCTGAGAGTCTGGTTGGTTATT). A plasmid containing the PDCoV S sequence was used to generate a standard curve. Cytokine mRNA levels were expressed as a ratio to the β-actin mRNA level. The specific primers for porcine IL-1β, IL-6, IL-12, TNF-α, IFN-α, IFN-β, Mx1, OAS, PKR and β-actin were designed with reference described previously [27,28] (Table 1). RT-qPCR was performed by an Applied Biosystems 7500 Fast Real-Time PCR System (Applied Biosystems, USA) using the TB Green™ Premix Ex Taq™ II (Tli RNaseH Plus) (TaKaRa, China).

### 2.14. Western blotting

The cells were lysed in radioimmunoprecipitation assay (RIPA) lysis buffer (CoWin Biosciences, China) with 100 U of proteinase inhibitors (CoWin Biosciences, China) and 20 μM NaF on ice for Western blotting assay. Primary antibodies used in this study were anti-PDCoV N (1:5, provided by Professor Pinghuang Liu, China Agricultural University, Beijing, China), anti-phospho-ERK, anti-phospho-JNK, anti-phospho-p38, anti-phospho-NF-κB p65 (1:500, Cell Signaling Technology, USA), anti-phospho-IκBα (1:300, Cell Signaling Technology, USA), anti-ERK, anti-JNK, anti-p38, anti-IκBα, anti-NF-κB (1:1000, Cell Signaling Technology, USA) and anti-β-actin (1:1000, ProteinTech Group, USA). Horseradish peroxidase conjugated to AffiniPure goat anti-mouse IgG (1:5000, ProteinTech Group, USA) or goat anti-rabbit IgG (1:5000, ProteinTech Group, USA) was used as secondary antibodies.

### 2.15. Statistical analysis

All experiments were performed 3 times. Statistical analysis was performed using IBM SPSS Statistics 25 software (IBM, USA). Differences between means were compared using Tukey's honestly significant difference post-hoc test. The data were visualized using GraphPad Prism 7 software (GraphPad Software, USA) and expressed as mean±standard deviation (SD). The statistically significant differences were set at $P < 0.05$. $^{*}P < 0.05$; $^{**}P < 0.01$; $^{***}P < 0.001$.

**Table 1**
Sequences of the primers used for RT-qPCR.

| Primers name | Direction[a] | Sequence (5′→3′) |
|---|---|---|
| IL-1β | F | AACGTGCAGTCTATGGAGT |
| | R | GAACACCACTTCTCTCTTCA |
| IL-6 | F | CTGGCAGAAAACA ACCTGAACC |
| | R | TGATTCTCATCAAGCAGGTCTCC |
| IL-12 | F | CGTGCCTCGGGCAATTATA |
| | R | CGCAGGTGAGGTCGCTAGTT |
| TNF-α | F | AACCTCAGATAAGCCCGTCG |
| | R | ACCACCAGCTGGTTGTCTTT |
| IFN-α | F | TCTCATGCACCAGAGCCA |
| | R | CCTGGACCACAGAAGGGA |
| IFN-β | F | AGTGCATCCTCCAAATCGCT |
| | R | GCTCATGGAAAGAGCTGTGGT |
| Mx1 | F | GGCGTGGGAATCAGTCATG |
| | R | AGGAAGGTCTATGAGGGTCAGATCT |
| OAS | F | GAGCTGCAGCGAGACTTCCT |
| | R | TGCTTGACAAGGCGGATGA |
| PKR | F | AAAGCGGACAAGTCGAAAGG |
| | R | TCCACTTCATTTCCATAGTCTTCTGA |
| β-actin | F | TGACTGACTACCTCATGAAGATCC |
| | R | TCTCCTTAATGTCACGCACGATT |

[a] F = forward; R = reverse.

## 3. Results

### 3.1. Cytotoxicity of ergosterol peroxide on LLC-PK1 cells

We obtained about 30 mg of EP ($C_{28}H_{44}O_3$, MW 428.65) with a purity of over 97% from 1,200 g of *C. volvatus*. The chemical structure of EP was shown in Fig. 1A. The relative cell viability was above 80% after treatment with EP at concentrations of 3.9, 7.8, 15.5, 31, 62, 124 and 248 μM for 36 h (Fig. 1B), respectively. Based on these results, 62, 124 and 248 μM were chosen as nontoxic EP concentrations for the subsequent antiviral assays.

### 3.2. Ergosterol peroxide inhibits PDCoV replication

To evaluate the antiviral activity of EP against PDCoV, LLC-PK1 cells were infected with PDCoV and treated with EP at concentrations of 62, 124 and 248 μM. The inhibitory effects of EP on PDCoV replication were assessed at 24 h post-infection (hpi). Western blotting analysis demonstrated that EP treatment decreased the amount of PDCoV N protein relative to mock-treated infected cells in a dose-dependent manner (Fig. 2A, B). In addition, the inhibitory effects of EP on PDCoV infection were confirmed by RT-qPCR (Fig. 2C), virus titration (Fig. 2D) and IFA (Fig. 2E, F). Compared with the mock-treated infected cells, the viral RNA copies were decreased by 2.6 and 1.6 logs in the 248 μM and the 124 μM EP-treated infected cells, respectively (Fig. 2C). The viral titers of infected cells treated with 248 μM or 124 μM EP were decreased by 4.52 or 3.49 $lgTCID_{50}$/mL, respectively as compared with the infected cells without EP (Fig. 2D). The IFA showed that EP treatment resulted in a significant dose-dependent reduction of infected cells (Fig. 2E, F). To further confirm its antiviral activity, we also characterized the inhibitory effects of EP on PDCoV replication in ST cells. The results were shown in Fig. S1, demonstrating that EP also reduced the number of infected cells efficiently. Taken together, these results demonstrate that EP has inhibitory effects on PDCoV.

### 3.3. Ergosterol peroxide inhibits different stages of the PDCoV replication cycle

The early events of the viral infection cycle include virus attachment and entry into cells. Here, we investigated whether EP blocked PDCoV attachment or entry into cells. The number of viral RNA copies in infected LLC-PK1 cells was significantly reduced by EP treatment ($P < 0.001$) in both attachment (Fig. 3A) and entry (Fig. 3B) assays. In addition, the inhibitory effect of 248 μM EP on viral replication was stronger than that of 124 μM EP.

Subsequently, we determined the role of EP in the post-entry stage of PDCoV infection. EP treatment led to a significant reduction of viral RNA copy numbers (Fig. 3C) ($P < 0.001$) and viral titers (Fig. 3D) ($P < 0.01$) relative to PDCoV-infected cells without EP treatment. In addition, the inhibitory effect of 248 μM EP on virus replication was greater than that of 124 μM EP. Furthermore, IFA results confirmed that EP treatment inhibited PDCoV infection at the post-entry stage (Fig. 3E, F).

To determine at which step(s) EP acts to mediate its antiviral effect in the post-entry stage of PDCoV, time-of-addition experiments were performed in LLC-PK1 cells (Fig. 4). The viral RNA copy numbers and the number of infected cells significantly decreased when the infected cells were treated with EP during 1–3 hpi (Fig. 4A, B, G) ($P < 0.001$) or 3–5 hpi (Fig. 4C, D, H) ($P < 0.001$) compared with mock-treated infected cells. In addition, the decreases were greater when the cells were treated with 248 μM EP compared with 124 μM EP ($P < 0.001$). However, there were no significant differences in PDCoV infection between EP- and mock-treated infected cells during 5–7 hpi as measured by the number of viral RNA copies or by the number of infected cells (Fig. 4E, F, I). These results suggest that EP mediates its antiviral effect at the early and middle stages of PDCoV replication.

### 3.4. Ergosterol peroxide directly inactivates PDCoV virions

To determine the viricidal effects of EP on PDCoV, we pretreated live PDCoV virions with various concentrations of EP at 37 ℃ for 2 h. We then washed and re-purified the virions, and tested their infectivity. Treatment of the virions with EP decreased viral infectivity compared with mock-treated virions as measured by mRNA levels (Fig. 5A) ($P < 0.001$), viral titers (Fig. 5B) (248 μM, $P < 0.001$; 124 μM, $P < 0.01$) and the number of infected cells (Fig. 5C, D). In addition, treatment with 248 μM EP was more effective in decreasing viral infectivity compared with 124 μM EP. To determine whether EP exerts an antiviral effect by pre-influencing host cells, we pretreated cells with EP for 2 h at 37 ℃ and infected the cells with PDCoV after washing them rigorously to remove residual EP. However, there was no significant difference in viral infectivity between EP- and mock-treated infected cells (Fig. 5E-H). These results indicate that EP can directly inactivate PDCoV virions, and preincubation of cells with EP has no inhibitory effect on virus replication.

### 3.5. Ergosterol peroxide inhibits LLC-PK1 cell apoptosis caused by PDCoV infection

PDCoV infection induces apoptosis in LLC-PK1 cells [29]. To determine the effect of EP treatment on apoptosis induced by PDCoV infection, the cells were infected with PDCoV and treated with EP for 36 h, at which time cells were assessed for apoptosis. At 36 hpi, PDCoV infection induced early and late apoptosis in 35.81% and 12.28% of cells, respectively (Fig. 6). PDCoV-induced apoptosis was decreased after EP treatment. The early and late apoptosis rates were 11.3% and 5.67% in 248 μM EP-treated cells, and 21.47% and 8.58% in 124 μM EP-treated

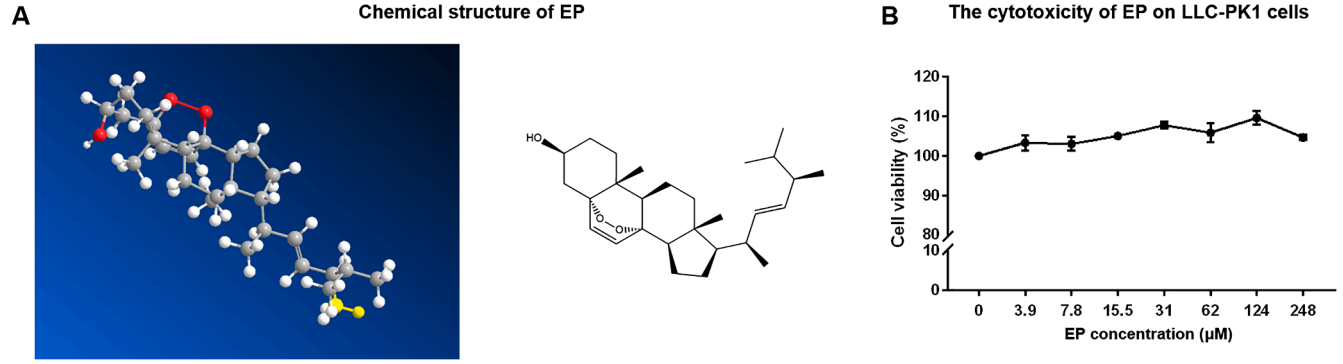


**Fig. 1.** The cytotoxicity of ergosterol peroxide on LLC-PK1 cells. A. Chemical structure of EP. B. Determination of cytotoxicity of EP by CCK8 assay. Cells were treated with 0, 3.9, 7.8, 15.6, 31, 62, 124 and 248 μM EP for 36 h, respectively. The relative cell viability was evaluated by CCK8 Kit according to the manufacturer's instructions. Values represent the mean ± SD for three independent experiments. $^*P < 0.05$; $^{**}P < 0.01$; $^{***}P < 0.001$.

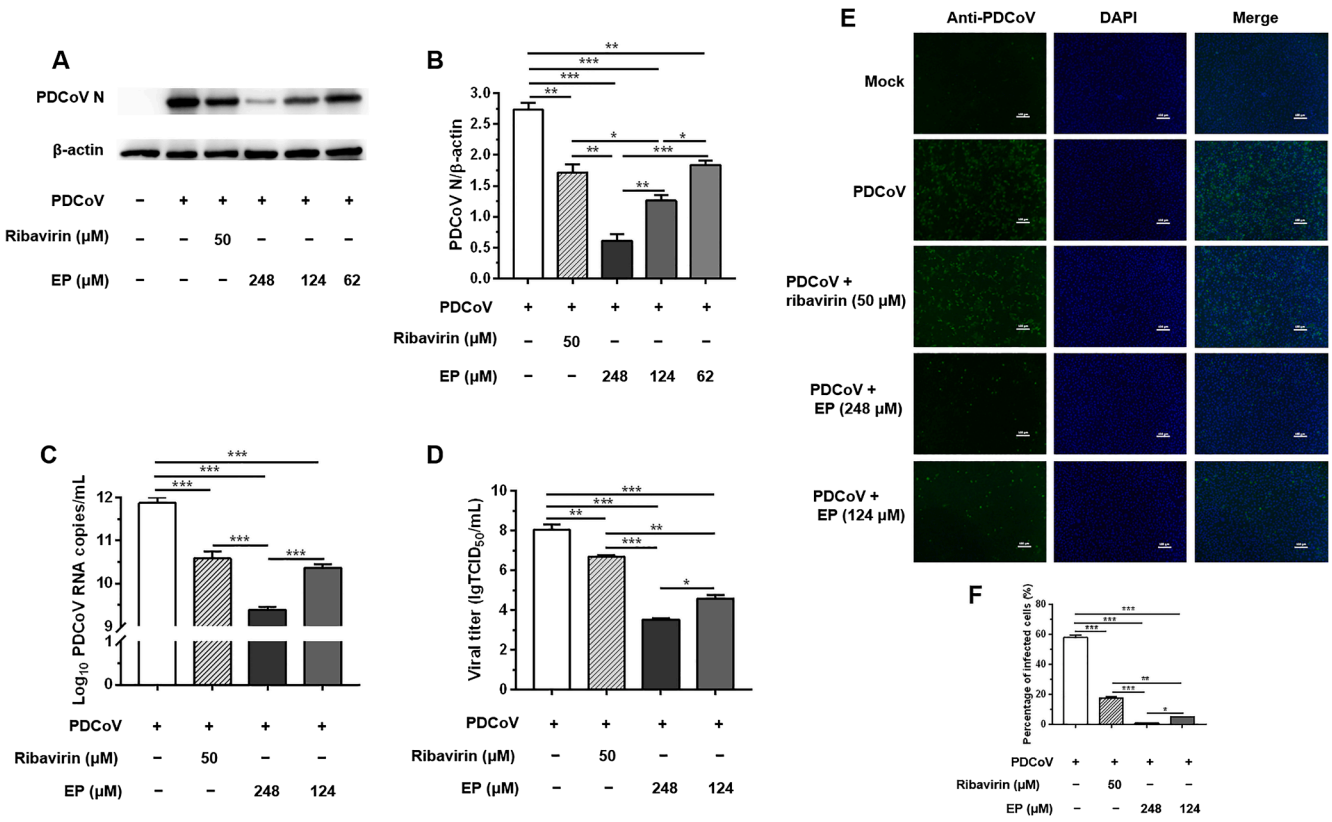


**Fig. 2.** Antiviral effect of ergosterol peroxide on PDCoV replication. A. The protein levels of PDCoV N in LLC-PK1cells were determined by Western blotting. B. Results were presented as the ratio of protein band intensity to the intensity of the β-actin band. C. The viral RNA copies in LLC-PK1 cells were determined by RT-qPCR with primers targeting the PDCoV S gene. D. The viral titer ($lgTCID_{50}$/mL) in LLC-PK1 supernatants was calculated by the method of Reed and Muench. E. PDCoV replication in LLC-PK1 cells was determined by IFA. Green fluorescence represents the PDCoV distribution, and the blue fluorescence represents the nuclear distribution. F. Percentage of infected cells in different treatment groups in E. Values represent the mean ± SD for three independent experiments. $^{*}P < 0.05$; $^{**}P < 0.01$; $^{***}P < 0.001$. Scale bars, 100 μm. (For interpretation of the references to colour in this figure legend, the reader is referred to the web version of this article.)

cells, respectively (Fig. 6). Therefore, EP treatment inhibits PDCoV-induced apoptosis *in vitro*.

### *3.6. Ergosterol peroxide inhibits PDCoV-induced mRNA expression of cytokines in LLC-PK1 cells*

Viral infections induce the release of cytokines, which may contribute to their pathogenesis. Studies have shown that PDCoV infection can induce the secretion of IL-6, IL-12, TNF-α, IFN-α and IFN-β *in vivo* [30,31]. Thus, we used RT-qPCR to determine whether treatment of LLC-PK1 cells with EP altered the expression of pro-inflammatory cytokines, type I interferons (IFN) and IFN-stimulated genes (ISGs) induced by PDCoV infection. As expected, PDCoV infection increased the mRNA expressions of IL-1β, IL-6, IL-12, TNF-α, IFN-α, IFN-β, Mx1 and PKR (Fig. 7A-G, I). However, EP treatment significantly reduced IL-1β, IL-6, IL-12, TNF-α, IFN-α, IFN-β, Mx1 and PKR expressions induced by PDCoV infection in a dose-dependent manner (Fig. 7A-G, I). In addition, we transfected LLC-PK1 cells with polyinosine-polycytidylic acid (polyI:C) followed by EP or mock treatment, and then analyzed the mRNA expression of cytokines. The results showed that EP remarkably reduced the mRNA levels of IL-1β, IL-6, IL-12, TNF-α, IFN-α, IFN-β, Mx1 and PKR up-regulated by polyI:C (Fig. 7A-G, I). These data demonstrate that EP can potentially regulate immune responses in PDCoV-infected cells by decreasing the mRNA expressions of cytokines.

### *3.7. Ergosterol peroxide suppresses PDCoV-induced activations of IκBα and p38 in LLC-PK1 cells*

A variety of CoVs have been reported to utilize the NF-κB and MAPK signaling pathways to promote their infection [21,22]. Here, we examined the impact of PDCoV infection on these two signaling pathways and determined whether the inhibition of PDCoV infection by EP was related to the signalings. Our data demonstrated that PDCoV infection induced the phosphorylation of IκBα (Fig. 8A, F), NF-κB p65 (Fig. 8B, G), ERK (Fig. 8C, H), JNK (Fig. 8D, I) and p38 (Fig. 8E, J). Treatment with EP significantly decreased the PDCoV-induced activations of IκBα (Fig. 8A, F) and p38 (Fig. 8E, J) in a dose-dependent manner. EP treatment did not decrease the phosphorylation of NF-κB p65 (Fig. 8B, G), ERK (Fig. 8C, H) or JNK (Fig. 8D, I). In fact, treatment with 124 μM EP increased the phosphorylation of NF-κB p65 (Fig. 8B, G), ERK (Fig. 8C, H) and JNK (Fig. 8D, I). Next, LLC-PK1 cells were transfected with polyI:C followed by EP treatment or mock treatment, and then the phosphorylation of IκBα was analyzed. The results showed that EP repressed IκBα phosphorylation induced by polyI:C (Fig. 9A, C). To explore whether EP affects PDCoV replication by inhibiting p38/MAPK signaling pathway, we treated LLC-PK1 cells with different concentrations of p38 inhibitor SB203580 for 1 h prior to infection. As shown in Fig. 9B, D, the p38 inhibitor reduced PDCoV N protein levels in a dose-dependent manner when compared with mock-treated PDCoV infected cells. Thus, the IκBα and p38/MAPK signaling pathways might be involved in the anti-PDCoV mechanisms of EP in LLC-PK1 cells.

## 4. Discussion

PDCoV is disseminated globally and results in significant economic losses to the pig industry. In addition, there are only a few reports on anti-PDCoV drugs and vaccines, highlighting the importance of identifying effective antiviral drugs. Natural products from Chinese herbs

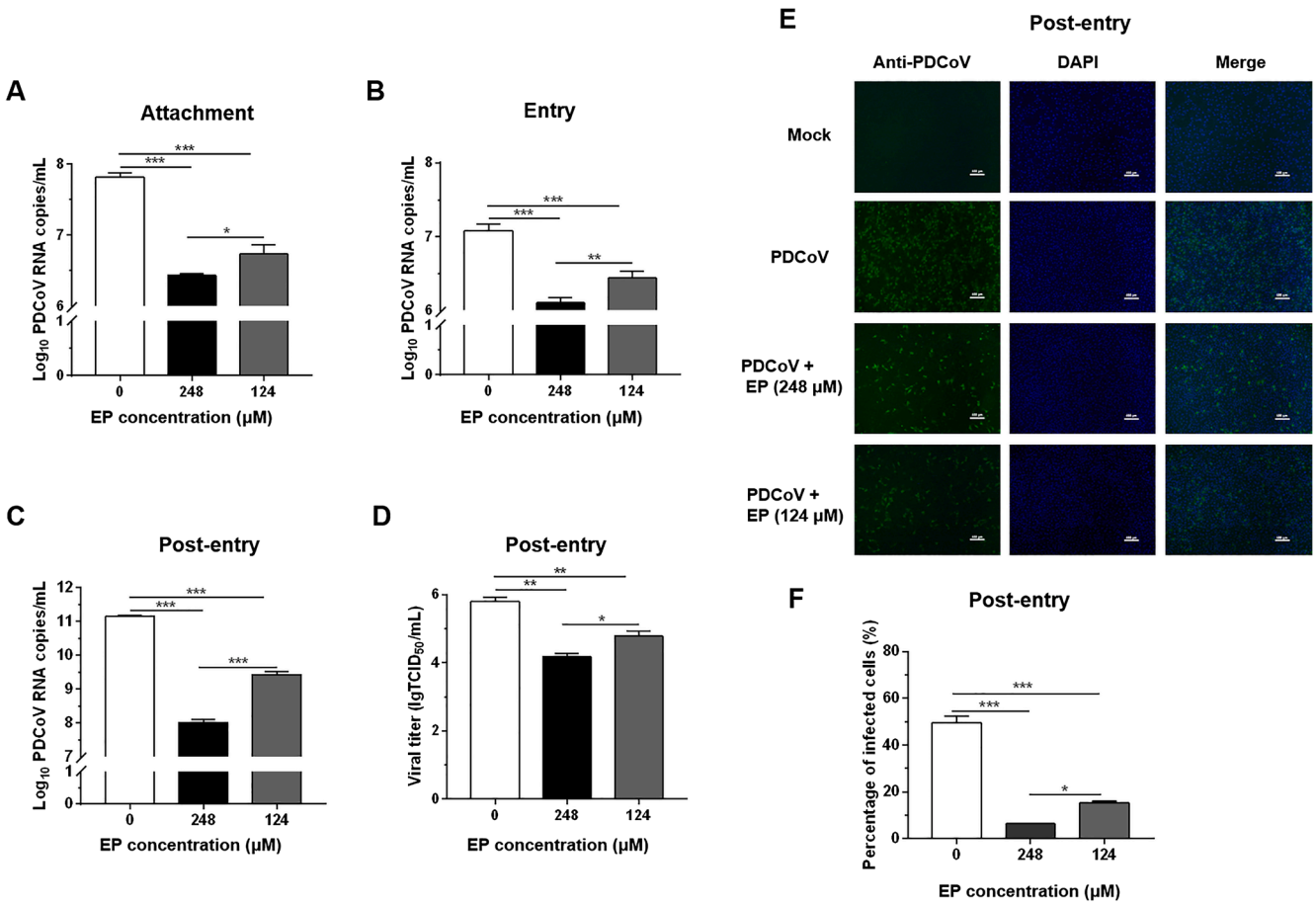


**Fig. 3.** Antiviral effect of ergosterol peroxide on different stages of PDCoV life cycle. The viral RNA copies in LLC-PK1 cells treated with various concentrations of EP during viral attachment (A), entry (B) and post-entry stage (C) were determined by RT-qPCR with primers targeting the PDCoV S gene. D. The viral titer ($lgTCID_{50}$/mL) in LLC-PK1 supernatants treated with different concentrations of EP in the post-entry stage was calculated by the method of Reed and Muench. E. Inhibitory effects of EP on PDCoV in the post-entry stage were observed by IFA. Green fluorescence represents the PDCoV distribution, and the blue fluorescence represents the nuclear distribution. F. Percentage of infected cells in different treatment groups in E. Values represent the mean ± SD for three independent experiments. $^{*}P < 0.05$; $^{**}P < 0.01$; $^{***}P < 0.001$. Scale bars, 100 μm. (For interpretation of the references to colour in this figure legend, the reader is referred to the web version of this article.)

have attracted the attention of pharmacists and have been exploited extensively in the pursuit of new antiviral agents. For example, the application of Traditional Chinese Medicine (TCM) for the treatment or prevention of SARS-CoV-2 and SARS-CoV has had an outstanding effect [32]. According to the National Administration of Traditional Chinese Medicine report, 214 SARS-CoV-2 patients were treated with *Qing Fei Pai Du Tang* and the overall effective rate was ≥ 90%. Mushrooms have been applied as TCM for centuries, and dried extracts from fruit bodies are a lucrative segment of the market for herbal medicines in western countries [33].

*C. volvatus*, which grows in certain areas of China, belongs to the family *Aphyllophorales* and the genus *Cryptoporus* [34]. Aqueous extracts from the fruiting body of *C. volvatus* have been reported to have multiple bioactivities, such as anti-tumorigenic, anti-allergic, anti-inflammatory and antiviral activities [35–37]. According to our previous studies, *C. volvatus* extract has potent antiviral properties against influenza virus and PRRSV [14,15,37,38]. Also, the chemical constituents of *C. volvatus* have been studied, and several compounds and their structures have been elucidated [23]. In the current study, we assessed the anti-PDCoV activity of EP from *C. volvatus* and found that EP efficiently inhibited PDCoV replication.

The replication of CoV begins with the attachment of viral particles to host cells and entry, which are essential early steps in the viral life cycle. The intervention strategies that block early viral attachment and entry are particularly effective for combating viral infections and the accompanying inflammatory diseases. Our data demonstrated that EP potently blocked PDCoV attachment and entry. Following entry, the viral particle is uncoated, which starts translation, transcription, RNA replication, protein synthesis, assembly, maturation and release. Interruptions to any of these processes can impair virus replication. In this study, EP also exerted its inhibitory effects on the post-entry stage of the PDCoV life cycle, and the time-of-addition assays indicated that the inhibition mainly took place at the early and middle stages of the PDCoV life cycle. The effective replication of the virus is dependent on the host cell machinery. CoV modulates several cellular pathways to enhance its replication by regulating the phosphorylation and dephosphorylation of host proteins, including the MAPK signaling pathway [21,39]. Our study demonstrated that PDCoV infection activated p38 signaling pathway, and its inhibitor inhibited PDCoV replication in a dose-dependent manner, suggesting that PDCoV may activate the p38/MAPK signaling pathway to facilitate its replication. Treatment with EP suppressed p38 activation induced by PDCoV infection. Therefore, we speculate that interfering with p38/MAPK signaling might be one of the anti-PDCoV mechanisms used by EP in LLC-PK1 cells. The p38/MAPK signaling pathway has been suggested to be involved in viral entry. The activation of p38 induced by the influenza virus can enhance endocytosis to facilitate virus entry [40]. In addition, inhibition of p38 has been reported to result in reduced PEDV RNA synthesis and protein expression during the post-entry steps of the PEDV life cycle [21]. Murine coronavirus utilizes increased p38 to phosphorylate eIF4E (a viral mRNA

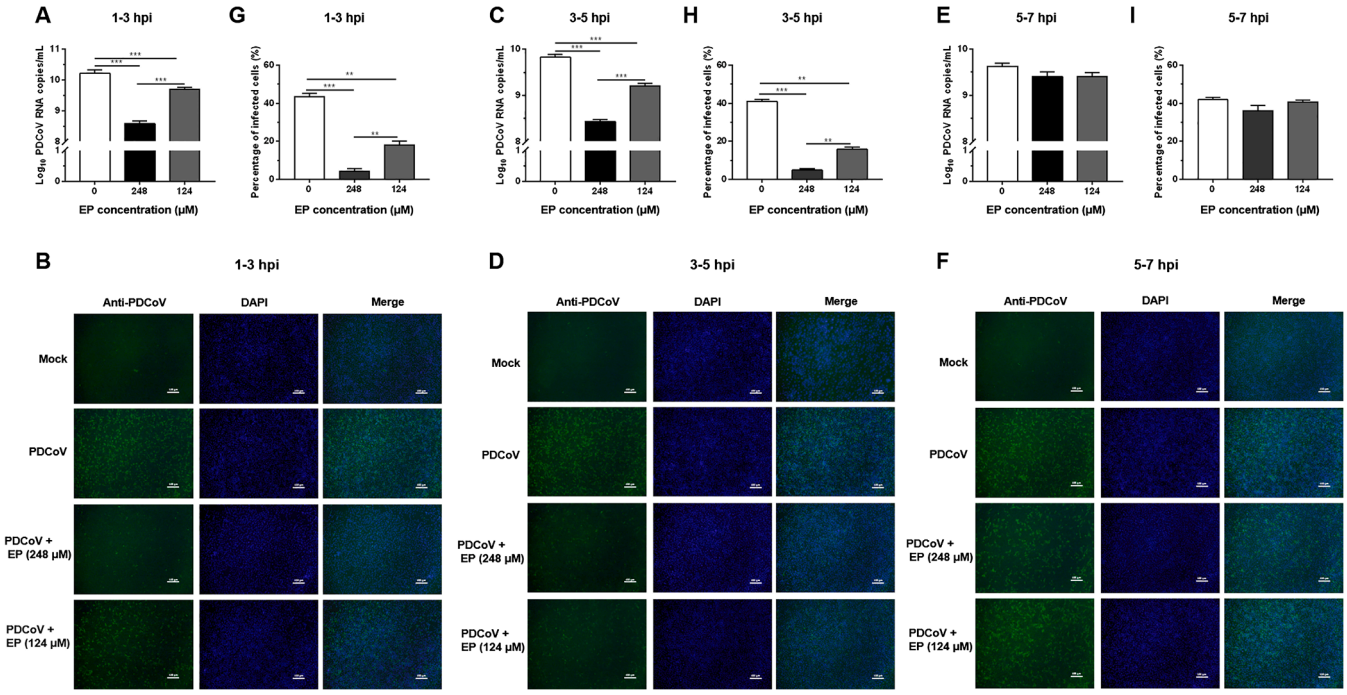


**Fig. 4.** Time-of-addition assays of the inhibitory effects of ergosterol peroxide on PDCoV replication. The inhibitory effects of EP on PDCoV during 1–3 hpi were determined by RT-qPCR (A) and IFA (B). The inhibitory effects of EP on PDCoV during 3–5 hpi were determined by RT-qPCR (C) and IFA (D). The inhibitory effects of EP on PDCoV during 5–7 hpi were determined by RT-qPCR (E) and IFA (F). G-I. Percentage of infected cells in different treatment groups in B, D and F. RT-qPCR was performed with primers targeting the PDCoV S gene. Green fluorescence represents the PDCoV distribution, and the blue fluorescence represents the nuclear distribution. Values represent the mean ± SD for three independent experiments. $^{*}P < 0.05$; $^{**}P < 0.01$; $^{***}P < 0.001$. Scale bars, 100 μm. (For interpretation of the references to colour in this figure legend, the reader is referred to the web version of this article.)

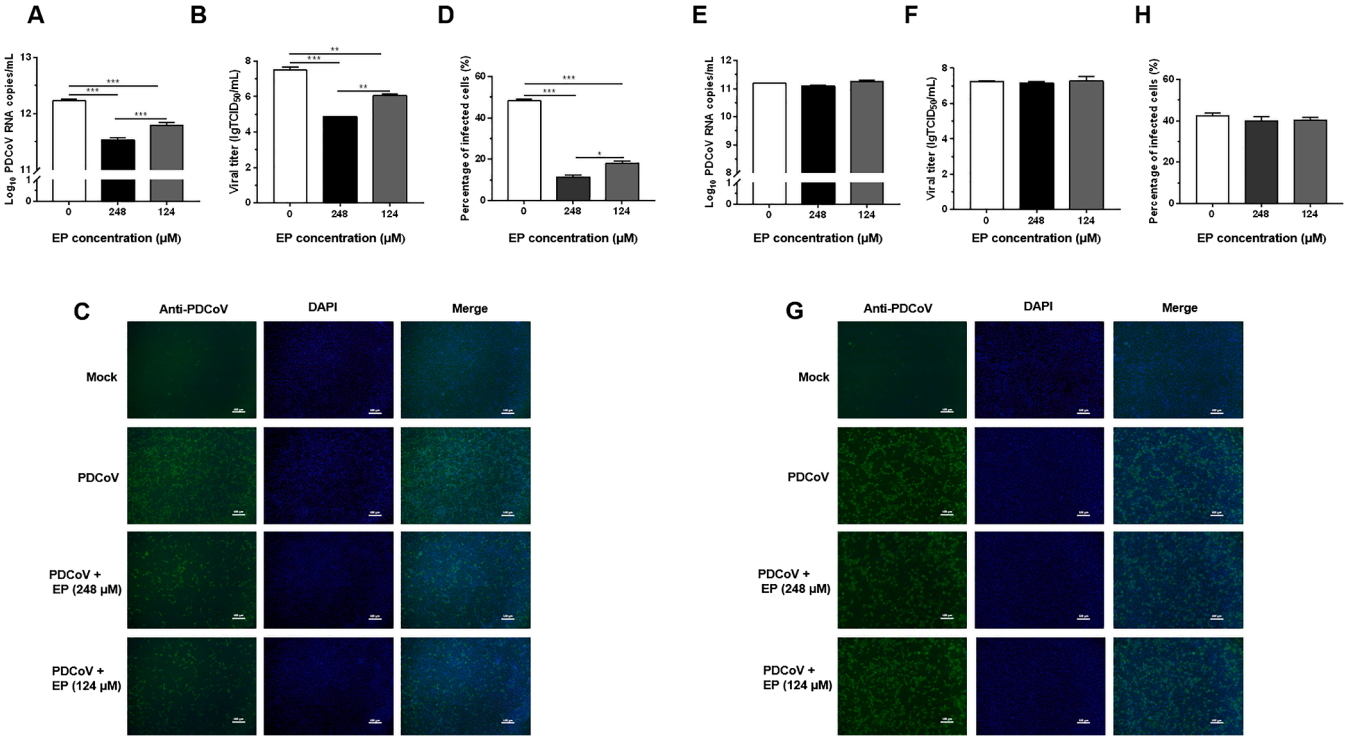


**Fig. 5.** Ergosterol peroxide directly inactivates PDCoV virions. The viricidal effect of EP on PDCoV was determined by RT-qPCR (A), viral titer ($lgTCID_{50}$/mL) (B) and IFA (C). The effect of preincubation of cells with EP for 2 h on PDCoV infection was determined by RT-qPCR (E), viral titer ($lgTCID_{50}$/ml) (F) and IFA (G). D, H. Percentage of infected cells in different treatment groups in C and G. RT-qPCR was performed with primers targeting the PDCoV S gene. Viral titer (lgTCID50/mL) in LLC-PK1 supernatant was calculated by the method of Reed and Muench. Green fluorescence represents the PDCoV distribution, and the blue fluorescence represents the nuclear distribution. Values represent the mean ± SD for three independent experiments. $^{*}P < 0.05$; $^{**}P < 0.01$; $^{***}P < 0.001$. Scale bars, 100 μm. (For interpretation of the references to colour in this figure legend, the reader is referred to the web version of this article.)

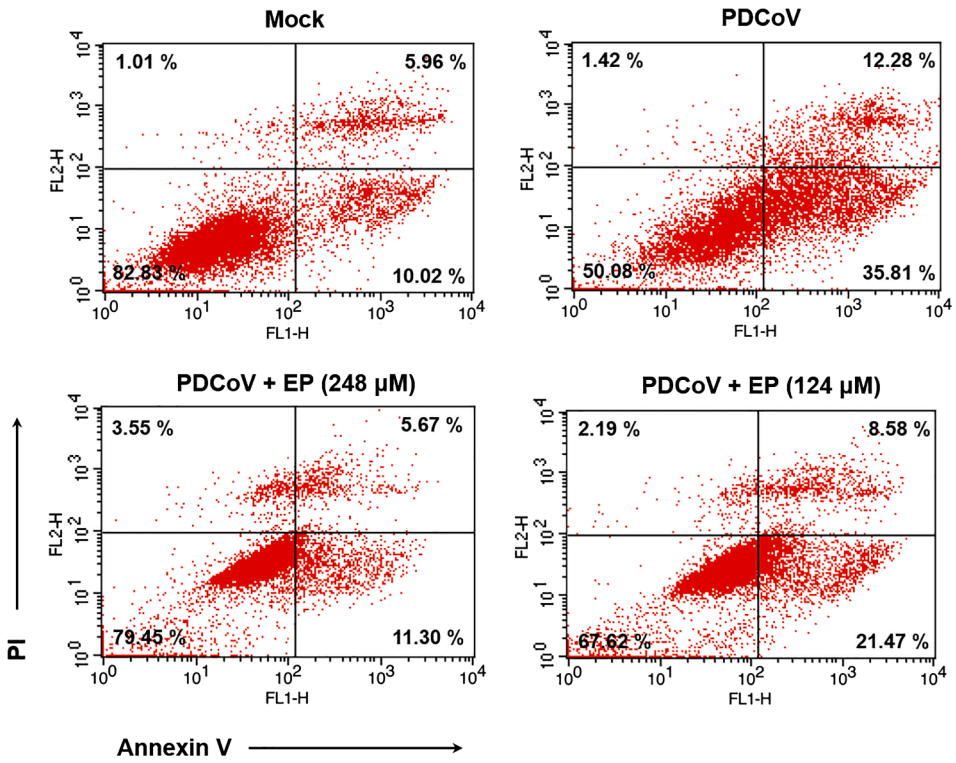


**Fig. 6.** Effect of ergosterol peroxide on apoptosis caused by PDCoV infection. Cells were incubated with PDCoV (MOI=0.5) for 1 h. Thereafter, the supernatant was removed, and MEM supplemented with various concentrations of EP was added. At 36 hpi, the rates of apoptosis were analyzed by flow cytometry.

translation factor) to promote virus-specific protein synthesis and subsequent progeny virus production [39]. Taken together, our data suggest that EP may inhibit PDCoV infection through the inhibition of the p38/MAPK signaling pathway. However, further study is required to elucidate the detailed mechanisms.

Although pre-incubation of host cells with EP at 37 ℃ for 2 h did not prevent PDCoV infection, pre-incubation of PDCoV virions with EP significantly suppressed PDCoV replication, implying that EP has a viricidal effect on PDCoV. These results are consistent with our previous study showing that Cryptoporic acid E from *C. volvatus* directly impaired influenza virus infectivity [38]. EP may disrupt the integrity of viral particles to achieve its viricidal effects. The integrity of viral particles is essential for preventing the viral genome from being exposed to RNase and degraded, which is pivotal to virus infectivity [41]. This inhibitory effect occurs before the virus invades the host cell and is a critical direction for the development of antiviral drugs.

A rapid well-coordinated innate immune response is the first line of defense against viral infections, but dysregulated and excessive immune responses may mediate immunopathology. Cytokines play important roles in immunity and immunopathology during viral infections. For example, acute lung injury caused by SARS-CoV or MERS-CoV infection is closely related to the elevated pro-inflammatory cytokine responses [42]. In addition, intensive immunosuppression reduces the mortality as a result of SARS-CoV-2-associated cytokine storm syndrome [43]. The NF-κB signaling pathway is a crucial mediator of cytokines and plays a central role in the host response to viral infections. In unstimulated cells, NF-κB complexes are inactive and reside predominantly in the cytoplasm with inhibitory IκB proteins. When the NF-κB signaling pathway is activated, the IκB protein is degraded, and NF-κB dimers translocate into the nucleus to modulate target gene expressions [44]. Persistent activation of the NF-κB signaling pathway could trigger inflammation by stimulating the expression of various cytokines [45]. The NF-κB signaling pathway is highly activated during infections with diverse CoVs, such as SARS-CoV and PEDV, leading to the excessive secretion of cytokines, acceleration of the pathogenesis and disease development [46,47]. Our results demonstrated that PDCoV activated the NF-κB signaling pathway as shown by the up-regulation of p-NF-κB p65 and p-IκBα in PDCoV-infected cells, which promotes the secretions of IL-1β, IL-6, IL-12, TNF-α, IFN-α, IFN-β, Mx1 and PKR. Treatment with EP reduced the mRNA expression of these cytokines and the protein expression of p-IκBα, while EP treatment did not reduce the protein expression of p-NF-κB p65. In addition, there is abundant evidence showing that p38 is involved in the secretion of pro-inflammatory cytokines. For example, feline infectious peritonitis virus increases the production of IL-1β and TNF-α in primary blood-derived feline mononuclear cells through the activation of the p38/MAPK signaling pathway [48]. Murine coronavirus-induced IL-6 can be repressed by a p38 inhibitor [39]. Therefore, we speculated that EP might suppress the overwhelming cytokines induced by PDCoV infection through inhibiting the phosphorylation of p38, IκBα and other transcription factors of the NF-κB family.

Cytokines are the key regulatory components in numerous apoptotic pathways [49,50]. The p38/MAPK signaling pathway also plays a critical role in triggering apoptosis [51]. Therefore, the remission of EP on the immoderate cytokine secretion and p38 activation caused by PDCoV infection might be crucial mechanisms by which EP inhibits PDCoV-induced apoptosis. Apoptosis is considered to be a host innate defense mechanism because it eliminates virus-infected cells. However, some viruses trigger apoptosis to facilitate the dissemination of viral progeny, which is one of the pathogenic properties of viruses that cause CPE *in vitro* and/or tissue injury *in vivo* [52]. Jejunum and ileum tissues infected with PDCoV exhibit acute diffuse, severe atrophic enteritis and moderate vacuolation and degeneration of enterocytes [1]. The massive loss of enterocytes hampers the absorption and digestion of nutrients and electrolytes in the small intestines, which causes malabsorptive and maldigestive diarrhea that consequently leads to fatal dehydration in piglets. Thus, the inhibition of PDCoV-induced apoptosis by EP may limit PDCoV infection and decrease the pathogenicity of PDCoV.

In conclusion, our findings revealed that EP could inhibit PDCoV infection in LLC-PK1 cells through targeting multiple stages of the

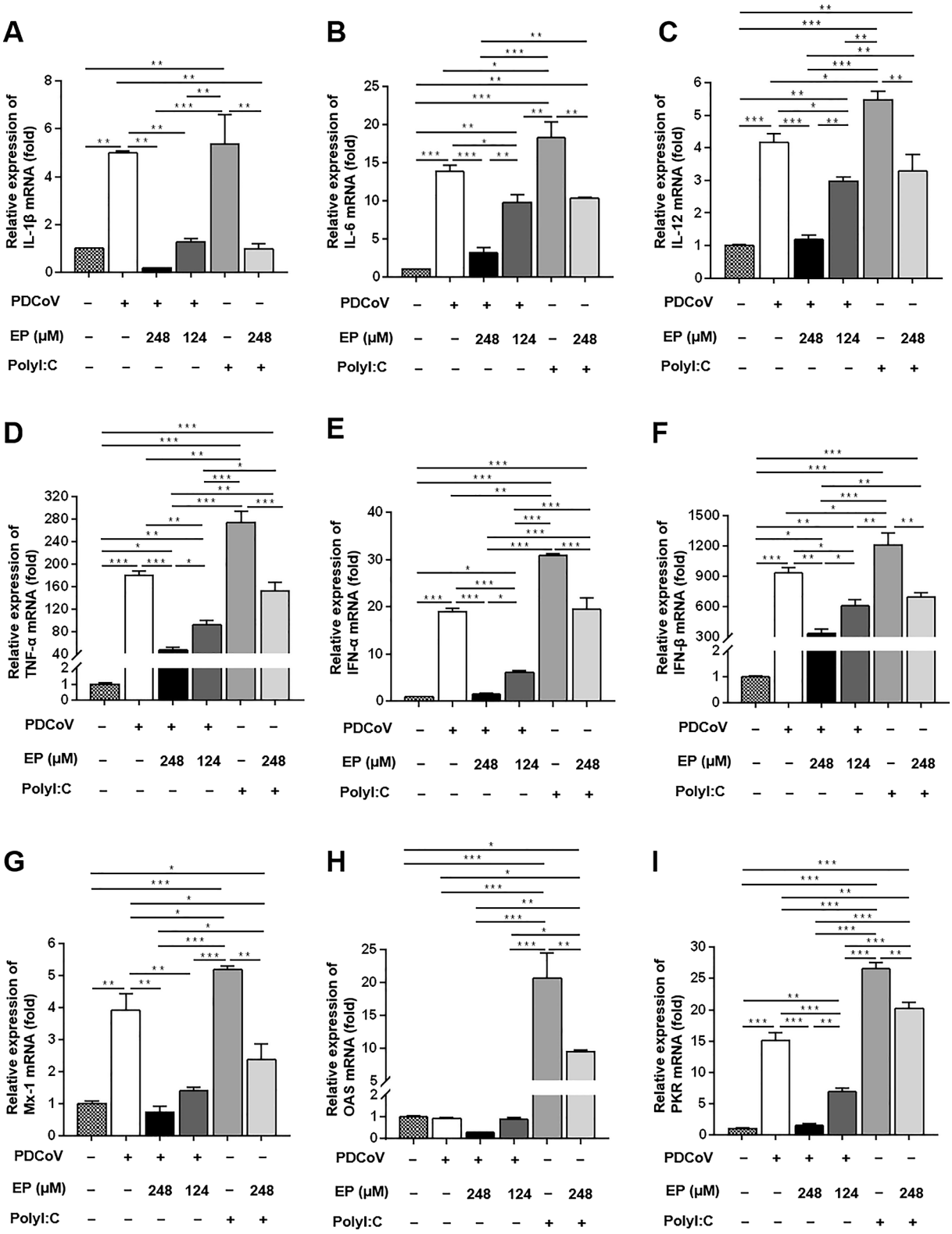


**Fig. 7.** Ergosterol peroxide alleviates PDCoV-induced mRNA expressions of cytokines in LLC-PK1 cells. LLC-PK1 cells were inoculated with PDCoV (MOI=0.5) or transfected with polyI:C in the presence or absence of EP. Total RNA was extracted from cell lysates at 24 hpi. The relative expression of IL-1β mRNA (A), IL-6 mRNA (B), IL-12 mRNA (C), TNF-α mRNA (D), IFN-α mRNA (E), IFN-β mRNA (F), Mx1 mRNA (G), OAS mRNA (H) and PKR mRNA (I) was assessed by RT-qPCR. Values represent the mean±SD for three independent experiments. $^{*}P < 0.05$; $^{**}P < 0.01$; $^{***}P < 0.001$.

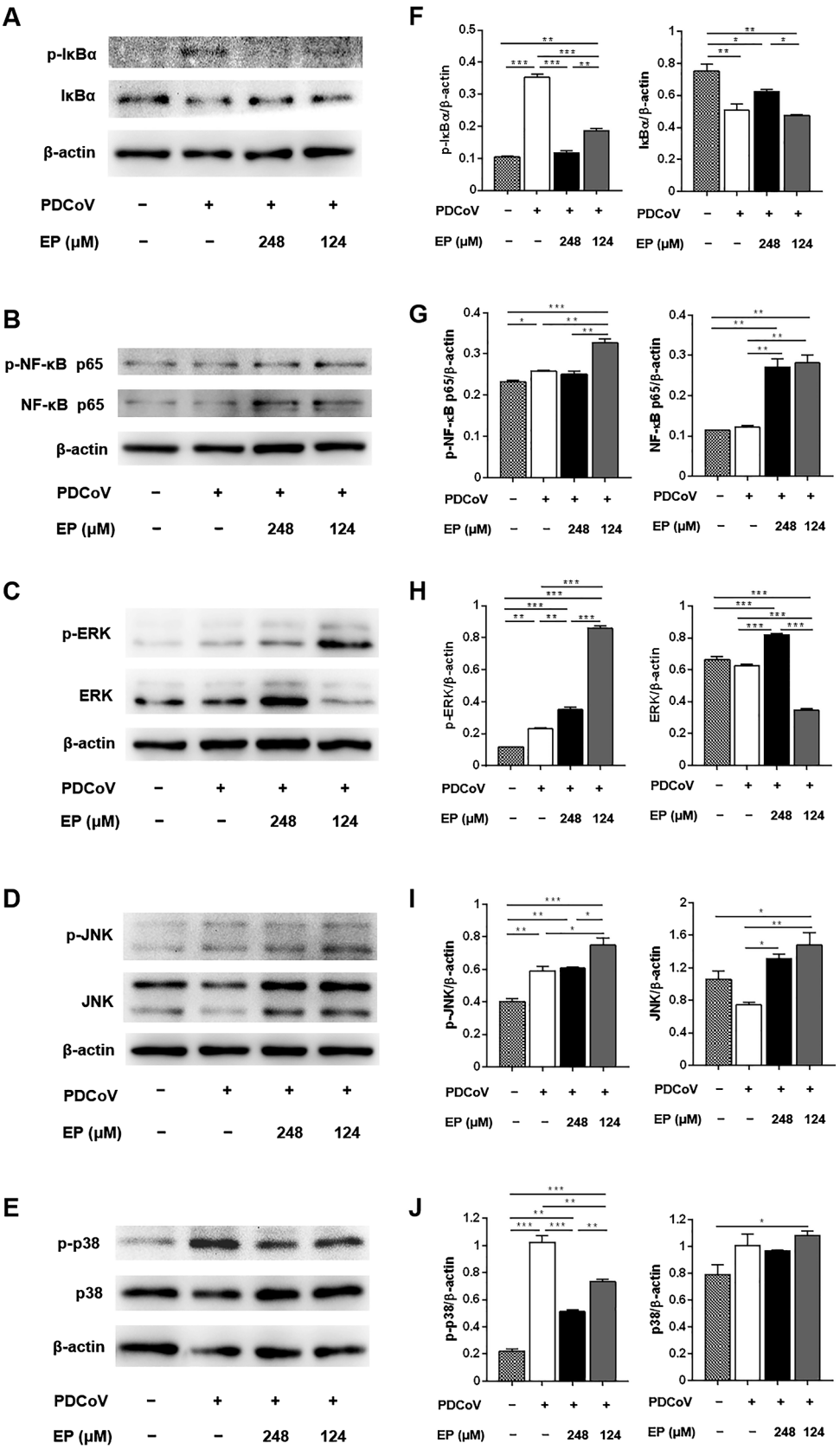


**Fig. 8.** Ergosterol peroxide suppresses PDCoV-induced activations of IκBα and p38 in LLC-PK1 cells. LLC-PK1 cells were inoculated with PDCoV (MOI = 0.5) in the presence or absence of EP. Western blotting analysis of p-IκBα and IκBα (A), p-NF-κB p65 and NF-κB p65 (B), p-ERK and ERK(C), p-JNK and JNK (D), p-p38 and p38 (E) was determined at 24 hpi. F-J. Results were presented as the ratio of protein band intensity to the intensity of the β-actin band. Values represent the mean±SD for three independent experiments. $^{*}P < 0.05$; $^{**}P < 0.01$; $^{***}P < 0.001$.

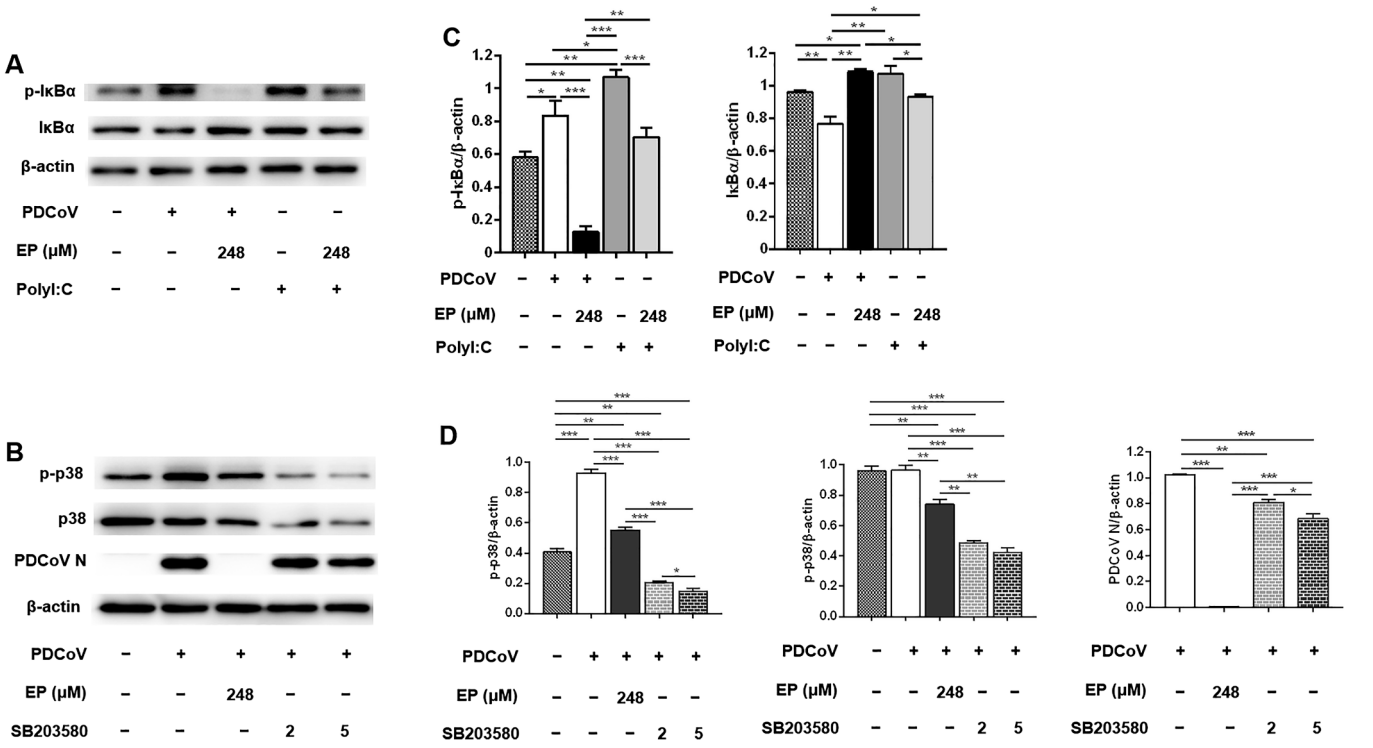


**Fig. 9.** The IκBα and p38/MAPK signaling pathways might be involved in the anti-PDCoV mechanisms of EP in LLC-PK1 cells. A. LLC-PK1 cells were inoculated with PDCoV (MOI=0.5) or transfected with polyI:C in the presence or absence of EP. Western blotting analysis of p-IκBα and IκBα was determined at 24 hpi. B. LLC-PK1 cells were pretreated with different concentrations of p38 inhibitor SB203580 for 1 h, followed by PDCoV infection (MOI=0.1) in the presence or absence of EP. Western blotting analysis of p-p38, p38 and PDCoV N was determined at 24 hpi. C, D. Results were presented as the ratio of protein band intensity to the intensity of the β-actin band. Values represent the mean ± SD for three independent experiments. $*P < 0.05$; $**P < 0.01$; $***P < 0.001$.

PDCoV life cycle, including attachment, entry and the early and middle stages of the post-entry stage. In addition, EP directly inactivated PDCoV infectivity and reduced early and late apoptosis caused by PDCoV infection. Furthermore, EP suppressed PDCoV-induced cytokines, including IL-1β, IL-6, IL-12, TNF-α, IFN-α, IFN-β, PKR and Mx1, and inhibited the activation of IκBα and p38 induced by PDCoV infection. Therefore, the antiviral and immunomodulatory abilities of EP against PDCoV may be attributed to the suppression of the NF-κB and p38/MAPK signaling pathways. These results provide some clues for the design of drugs against PDCoV.

## Declaration of Competing Interest

The authors declare that they have no known competing financial interests or personal relationships that could have appeared to influence the work reported in this paper.

*Acknowledgements*

We would like to thank the editor of MogoEdit for editing the manuscript. This study was supported by the National Key R&D Program of China (grant number 2017YFD0502200).

*Availability of data and materials*

All data generated or analyzed during this study can be made available by the corresponding author upon reasonable request.

*Consent for publication*

Not applicable.

## Appendix A. Supplementary material

Supplementary data to this article can be found online at https://doi.org/10.1016/j.intimp.2020.107317.

## References

[1] H. Hu, K. Jung, A.N. Vlasova, L.J. Saif, Experimental infection of gnotobiotic pigs with the cell-culture-adapted porcine deltacoronavirus strain OH-FD22, Arch. Virol. 161 (2016) 3421–3434, https://doi.org/10.1007/s00705-016-3056-8.
[2] P.C. Woo, S.K.P. Lau, C.S.F. Lam, C.C.Y. Lau, A.K.L. Tsang, J.H.N. Lau, R. Bai, J.L. L. Teng, C.C.C. Tsang, M. Wang, B.J. Zheng, K.H. Chan, K.Y. Yuen, Discovery of seven novel mammalian and avian coronaviruses in the genus deltacoronavirus supports bat coronaviruses as the gene source of alphacoronavirus and betacoronavirus and avian coronaviruses as the gene source of gammacoronavirus and deltacoronavirus, J. Virol. 86 (2012) 3995–4008, https://doi.org/10.1128/JVI.06540-11.
[3] G. Jang, K.K. Lee, S.H. Kim, C. Lee, Prevalence, complete genome sequencing and phylogenetic analysis of porcine deltacoronavirus in South Korea, 2014–2016, Transbound Emerg. Dis. 64 (2017) 1364–1370, https://doi.org/10.1111/tbed.12690.
[4] T. Ajayi, R. Dara, M. Misener, T. Pasma, L. Moser, Z. Poljak, Herd-level prevalence and incidence of porcine epidemic diarrhoea virus (PEDV) and porcine deltacoronavirus (PDCoV) in swine herds in Ontario, Canada, Transbound Emerg. Dis. 65 (2018) 1197–1207, https://doi.org/10.1111/tbed.12858.
[5] T. Suzuki, T. Shibahara, N. Imai, T. Yamamoto, S. Ohashi, Genetic characterization and pathogenicity of Japanese porcine deltacoronavirus, Infect. Genet. Evol. 61 (2018) 176–182, https://doi.org/10.1016/j.meegid.2018.03.030.
[6] N. Dong, L. Fang, H. Yang, H. Liu, T. Du, P. Fang, D. Wang, H. Chen, S. Xiao, Isolation, genomic characterization, and pathogenicity of a Chinese porcine deltacoronavirus strain CHN-HN-2014, Vet. Microbiol. 196 (2016) 98–106, https://doi.org/10.1016/j.vetmic.2016.10.022.
[7] K. Jung, H. Hu, L.J. Saif, Calves are susceptible to infection with the newly emerged porcine deltacoronavirus, but not with the swine enteric alphacoronavirus, porcine epidemic diarrhea virus, Arch. Virol. 162 (2017) 2357–2362, https://doi.org/10.1007/s00705-017-3351-z.
[8] Q. Liang, H. Zhang, B. Li, Q. Ding, Y. Wang, W. Gao, D. Guo, Z. Wei, H. Hu, Susceptibility of chickens to porcine deltacoronavirus infection, Viruses 11 (2019) 573, https://doi.org/10.3390/v11060573.
[9] P.A. Boley, M.A. Alhamo, G. Lossie, K.K. Yadav, M. Vasquez-Lee, L.J. Saif, S. P. Kenney, Porcine deltacoronavirus infection and transmission in poultry United

States, Emerg. Infect. Dis. 26 (2020) 255–265, https://doi.org/10.3201/eid2602.190346.
[10] Y. Shi, Y. Wu, W. Zhang, J. Qi, G.F. Gao, Enabling the 'host jump': structural determinants of receptor-binding specificity in influenza A viruses, Nat. Rev. Microbiol. 12 (2014) 822–831, https://doi.org/10.1038/nrmicro3362.
[11] H.L. Yen, E. Hoffmann, G. Taylor, C. Scholtissek, A.S. Monto, R.G. Webster, E. A. Govorkova, Importance of neuraminidase active-site residues to the neuraminidase inhibitor resistance of influenza viruses, J. Virol. 80 (2006) 8787–8795, https://doi.org/10.1128/JVI.00477-06.
[12] A.L. Harvey, Natural products in drug discovery, Drug. Discov. Today 13 (2008) 894–901, https://doi.org/10.1016/j.drudis.2008.07.004.
[13] U. Lindequist, T.H.J. Niedermeyer, W.D. Jülich, The pharmacological potential of mushrooms, Evid. Based Complement Alternat. Med. 2 (2005) 285–299, https://doi.org/10.1093/ecam/neh107.
[14] L. Gao, W. Zhang, Y. Sun, J. Ren, J. Liu, H. Wang, W.H. Feng, *Cryptoporus volvatus* extract inhibits porcine reproductive and respiratory syndrome virus (PRRSV) *in vitro* and *in vivo*, PLoS One 8 (2013) e63767, https://doi.org/10.1371/journal.pone.0063767.
[15] L. Gao, Y. Sun, J. Si, J. Liu, G. Sun, X. Sun, L. Cao, *Cryptoporus volvatus* extract inhibits influenza virus replication *in vitro* and *in vivo*, PLoS One 9 (2014) e113604, https://doi.org/10.1371/journal.pone.0113604.
[16] L. Ma, H. Chen, P. Dong, X. Lu, Anti-inflammatory and anticancer activities of extracts and compounds from the mushroom Inonotus obliquus, Food Chem. 139 (2013) 503–508, https://doi.org/10.1016/j.foodchem.2013.01.030.
[17] M. He, D. Su, Q. Liu, W. Gao, Y. Kang, Mushroom lectin overcomes hepatitis B virus tolerance *via* TLR6 signaling, Sci. Rep. 7 (2017) 5814, https://doi.org/10.1038/s41598-017-06261-5.
[18] T. Kawai, S. Akira, Pathogen recognition with Toll-like receptors, Curr. Opin. Immunol. 17 (2005) 338–344, https://doi.org/10.1016/j.coi.2005.02.007.
[19] J. Kindrachuk, B. Ork, B.J. Hart, S. Mazur, M.R. Holbrook, M.B. Frieman, D. Traynor, R.F. Johnson, J. Dyall, J.H. Kuhn, G.G. Olinger, L.E. Hensley, P. B. Jahrling, Antiviral potential of ERK/MAPK and PI3K/AKT/mTOR signaling modulation for Middle East respiratory syndrome coronavirus infection as identified by temporal kinome analysis, Antimicrob. Agents Chemother. 59 (2015) 1088–1099, https://doi.org/10.1128/AAC.03659-14.
[20] B. Hemonnot, C. Cartier, B. Gay, S. Rebuffat, M. Bardy, C. Devaux, V. Boyer, L. Briant, The host cell MAP kinase ERK-2 regulates viral assembly and release by phosphorylating the $p6^{gag}$ protein of HIV-1, J. Biol. Chem. 279 (2004) 32426–32434, https://doi.org/10.1074/jbc.M313137200.
[21] C. Lee, Y. Kim, J.H. Jeon, JNK and p38 mitogen-activated protein kinase pathways contribute to porcine epidemic diarrhea virus infection, Virus Res. 222 (2016) 1–12, https://doi.org/10.1016/j.virusres.2016.05.018.
[22] Q. Ma, W. Pan, R. Li, B. Liu, C. Li, Y. Xie, Z. Wang, J. Zhao, H. Jiang, J. Huang, Y. Shi, J. Dai, K. Zheng, X. Li, Z. Yang, Liu Shen capsule shows antiviral and anti-inflammatory abilities against novel coronavirus SARS-CoV-2 *via* suppression of NF-κB signaling pathway, Pharmacol. Res. 158 (2020), 104850, https://doi.org/10.1016/j.phrs.2020.104850.
[23] J. Wang, G. Li, N. Lv, L. Cao, L. Shen, J. Si, Chemical constituents from the fruiting bodies of *Cryptoporus volvatus*, Arch. Pharm. Res. 39 (2016) 747–754, https://doi.org/10.1007/s12272-016-0754-4.
[24] H. Hu, K. Jung, A.N. Vlasova, J. Chepngeno, Z. Lu, Q. Wang, L.J. Saif, Isolation and characterization of porcine deltacoronavirus from pigs with diarrhea in the United States, J. Clin. Microbiol. 53 (2015) 1537–1548, https://doi.org/10.1128/JCM.00031-15.
[25] L.J. Reed, H. Muench, A simple method of estimating fifty percent endpoints, Am. J. Hyg. 7 (1938) 493–497.
[26] D. Falzarano, E.D. Wit, A.L. Rasmussen, F. Feldmann, A. Okumura, D.P. Scott, D. Brining, T. Bushmaker, C. Martellaro, L. Baseler, A.G. Benecke, M.G. Katze, V. J. Munster, H. Feldmann, Treatment with interferon-α2b and ribavirin improves outcome in MERS-CoV–infected rhesus macaques, Nat. Med. 19 (2013) 1313–1317, https://doi.org/10.1038/nm.3362.
[27] D.P. Gladue, J. Zhu, L.G. Holinka, I. Fernandez-Sainz, C. Carrillo, M.V. Prarat, V. O'Donnell, M.V. Borca, Patterns of gene expression in swine macrophages infected with classical swine fever virus detected by microarray, Virus Res. 151 (2010) 10–18, https://doi.org/10.1016/j.virusres.2010.03.007.
[28] H. Hao, L. Wen, J. Li, Y. Wang, B. Ni, R. Wang, X. Wang, M. Sun, H. Fan, X. Mao, LiCl inhibits PRRSV infection by enhancing Wnt/β-catenin pathway and suppressing inflammatory responses, Antiviral Res. 117 (2015) 99–109, https://doi.org/10.1016/j.antiviral.2015.02.010.
[29] K. Jung, H. Hu, L.J. Saif, Porcine deltacoronavirus induces apoptosis in swine testicular and LLC porcine kidney cell lines *in vitro* but not in infected intestinal enterocytes *in vivo*, Vet. Microbiol. 182 (2016) 57–63, https://doi.org/10.1016/j.vetmic.2015.10.022.
[30] K. Jung, A. Miyazaki, H. Hu, L.J. Saif, Susceptibility of porcine IPEC-J2 intestinal epithelial cells to infection with porcine deltacoronavirus (PDCoV) and serum cytokine responses of gnotobiotic pigs to acute infection with IPEC-J2 cell culture-passaged PDCoV, Vet. Microbiol. 221 (2018) 49–58, https://doi.org/10.1016/j.vetmic.2018.05.019.
[31] Z. Xu, H. Zhong, S. Huang, Q. Zhou, Y. Du, L. Chen, C. Xue, Y. Cao, Porcine deltacoronavirus induces TLR3, IL-12, IFN-α, IFN-β and PKR mRNA expression in infected Peyer's patches *in vivo*, Vet. Microbiol. 228 (2019) 226–233, https://doi.org/10.1016/j.vetmic.2018.12.012.
[32] Y. Yang, M.S. Islam, J. Wang, Y. Li, X. Chen, Traditional Chinese Medicine in the treatment of patients infected with 2019-new Coronavirus (SARS-CoV-2): A review and perspective, Int. J. Biol. Sci. 16 (2020) 1708–1717, https://doi.org/10.7150/ijbs.45538.
[33] C. Gründemann, J.K. Reinhardt, U. Lindequist, European medicinal mushrooms: Do they have potential for modern medicine? - An update, Phytomedicine 66 (2020), 153131, https://doi.org/10.1016/j.phymed.2019.153131.
[34] Q. Hua, J. Sun, L. Shen, Biological characteristics of *Cryptoporus volvatus* (peck) Hubb., a medicinal fungus, Zhongguo Zhong Yao Za Zhi 16 (1991) 719–722, 761.
[35] Q.M. Xie, J.F. Deng, Y.M. Deng, C.S. Shao, H. Zhang, C.K. Ke, Effects of cryptoporus polysaccharide on rat allergic rhinitis associated with inhibiting eotaxin mRNA expression, J. Ethnopharmacol. 107 (2006) 424–430, https://doi.org/10.1016/j.jep.2006.03.040.
[36] J.P. Zhu, K. Wu, J.Y. Li, Y. Guan, Y.H. Sun, W.J. Ma, Q.M. Xie, *Cryptoporus volvatus* polysaccharides attenuate LPS-induced expression of pro-inflammatory factors via the TLR2 signaling pathway in human alveolar epithelial cells, Pharm. Biol. 54 (2016) 347–353, https://doi.org/10.3109/13880209.2015.1042981.
[37] Z. Ma, W. Zhang, L. Wang, M. Zhu, H. Wang, W.H. Feng, T.B. Ng, A novel compound from the mushroom *Cryptoporus volvatus* inhibits porcine reproductive and respiratory syndrome virus (PRRSV) *in vitro*, PLoS One 8 (2013), e79333, https://doi.org/10.1371/journal.pone.0079333.
[38] L. Gao, J. Han, J. Si, J. Wang, H. Wang, Y. Sun, Y. Bi, J. Liu, L. Cao, Cryptoporic acid E from *Cryptoporus volvatus* inhibits influenza virus replication *in vitro*, Antiviral Res. 143 (2017) 106–112, https://doi.org/10.1016/j.antiviral.2017.02.010.
[39] S. Banerjee, K. Narayanan, T. Mizutani, S. Makino, Murine coronavirus replication-induced p38 mitogen-activated protein kinase activation promotes interleukin-6 production and virus replication in cultured cells, J. Virol. 76 (2002) 5937–5948, https://doi.org/10.1128/jvi.76.12.5937-5948.2002.
[40] D. Marchant, G.K. Singhera, S. Utokaparch, T.L. Hackett, J.H. Boyd, Z. Luo, X. Si, D.R. Dorscheid, B.M. McManus, R.G. Hegele, Toll-like receptor 4-mediated activation of p38 mitogen-activated protein kinase is a determinant of respiratory virus entry and tropism, J. Virol. 84 (2010) 11359–11373, https://doi.org/10.1128/JVI.00804-10.
[41] G. Cheng, A. Montero, P. Gastaminza, C. Whitten-Bauer, S.F. Wieland, M. Isogawa, B. Fredericksen, S. Selvarajah, P.A. Gallay, M.R. Ghadiri, F.V. Chisari, A virocidal amphipathic α-helical peptide that inhibits hepatitis C virus infection *in vitro*, Proc. Natl. Acad. Sci. U S A 105 (2008) 3088–3093, https://doi.org/10.1073/pnas.0712380105.
[42] F. Channappanavar, S. Perlman, Pathogenic human coronavirus infections: causes and consequences of cytokine storm and immunopathology, Semin. Immunopathol. 39 (2017) 529–539, https://doi.org/10.1007/s00281-017-0629-x.
[43] S. Mayor, Intensive immunosuppression reduces deaths in covid-19-associated cytokine storm syndrome, study finds, BMJ 370 (2020), m2935, https://doi.org/10.1136/bmj.m2935.
[44] M.S. Hayden, S. Ghosh, NF-κB in immunobiology, Cell Res. 21 (2011) 223–244, https://doi.org/10.1038/cr.2011.13.
[45] M.G. Santoro, A. Rossi, C. Amici, NF-kappaB and virus infection: who controls whom, EMBO J. 22 (2003) 2552–2560, https://doi.org/10.1093/emboj/cdg267.
[46] M.L. DeDiego, J.L. Nieto-Torres, J.A. Regla-Nava, J.M. Jimenez-Guardeño, R. Fernandez-Delgado, C. Fett, C. Castaño-Rodriguez, S. Perlman, L. Enjuanes, Inhibition of NF-κB-mediated inflammation in severe acute respiratory syndrome coronavirus-infected mice increases survival, J. Virol. 88 (2014) 913–924, https://doi.org/10.1128/JVI.02576-13.
[47] L. Cao, X. Ge, Y. Gao, Y. Ren, X. Ren, G. Li, Porcine epidemic diarrhea virus infection induces NF-κB activation through the TLR2, TLR3 and TLR9 pathways in porcine intestinal epithelial cells, J. Gen. Virol. 96 (2015) 1757–1767, https://doi.org/10.1099/vir.0.000133.
[48] A.D. Regan, R.D. Cohen, G.R. Whittaker, Activation of p38 MAPK by feline infectious peritonitis virus regulates pro-inflammatory cytokine production in primary blood-derived feline mononuclear cells, Virology 384 (2009) 135–143, https://doi.org/10.1016/j.virol.2008.11.006.
[49] N. Tanaka, M. Sato, M.S. Lamphier, H. Nozawa, E. Oda, S. Noguchi, R.D. Schreiber, Y. Tsujimoto, T. Taniguchi, Type I interferons are essential mediators of apoptotic death in virally infected cells, Genes Cells 3 (1998) 29–37, https://doi.org/10.1046/j.1365-2443.1998.00164.x.
[50] Z. Luo, R. Su, W. Wang, Y. Liang, X. Zeng, M.A. Shereen, N. Bashir, Q. Zhang, L. Zhao, K. Wu, Y. Liu, J. Wu, EV71 infection induces neurodegeneration via activating TLR7 signaling and IL-6 production, PLoS Pathog. 15 (2019), e1008142, https://doi.org/10.1371/journal.ppat.1008142.
[51] P. Lin, Y. Cheng, S. Song, J. Qiu, L. Yi, Z. Cao, J. Li, S. Cheng, J. Wang, Viral nonstructural protein 1 induces mitochondrion-mediated apoptosis in mink enteritis virus infection, J. Virol. 93 (2019) e01249–19, https://doi.org/10.1128/JVI.01249-19.
[52] P. Clarke, K.L. Tyler, Apoptosis in animal models of virus-induced disease, Nat. Rev. Microbiol. 7 (2009) 144–155, https://doi.org/10.1038/nrmicro2071.